Inverting the Cellular Yule-Nielsen modified Spectral Neugebauer Model

Philipp Urban, Mitchell R. Rosen

Munsell Color Science Laboratory, Chester F. Carlson Center for Imaging Science,

Rochester Institute of Technology,

54 Lomb Memorial Drive, Rochester, New York 14623

Abstract

The cellular Yule-Nielsen modified spectral Neugebauer (CYNSN) model is widely used to predict the spectral response of inkjet printers. Inversion of the model is often implemented as a constrained optimization problem minimizing the difference between a desired reflectance and a model-predicted one. Inversion of CYNSN is considered to be computationally expensive. The Linear Regression Iteration (LRI) algorithm, already effectively used for the inversion of the simple YNSN model, is investigated as an efficient optimization method for inverting CYNSN. The proposed approach introduces a novel means for transitioning optimized choices from one cell to the neighboring cell. These transitions ensure the global consistency of the results. The matrices used by the LRI method can be calculated in advance for each cell and then arranged in a special scheme to allow fast access. This precalculated matrix scheme vastly increases the speed of inversion by reducing the algorithm to two simple steps for each iteration: choice of correct matrix and two simple matrix-vector multiplications.

Introduction

Maintaining spectral accuracy when printing a multispectral image requires the ability to choose suitable printer control values that produce appropriate spectral reflectances on the medium. This process is called spectral separation and often requires the inversion of an adequate printer model. The forward model is a prediction function, from control value space into spectral space. Various Printer models have been proposed in the past. Wybel and Berns[1] give an overview of common printer models.

Because of its simplicity and accuracy the Yule-Nielson modified spectral Neugebauer model (YNSN) is widely used in practice. Neugebauer's colorimetric model[2,3] was modified by Yule *et al.*[4,5] to consider optical dot gain. Viggiano applied the idea to the spectral case[6,7].

To further improve the spectral accuracy of the YNSN model more measurements than the Neugebauer primaries can be considered (Heuberger et al.[8]). For this reason the control value space can be subdivided into cells and the YNSN model can be applied in each cell utilizing the cell corners as primaries in place of the Neugebauer primaries. The location of the additional primaries can be optimized to minimize the maximal spectral RMS error (see Chen et al.[9])

Unfortunately, an analytical inversion of the cellular Yule-Nielsen modified spectral Neugebauer model (CYNSN) is not possible. Therefore, iterative inversion methods have to be used. An additional problem is the limited spectral gamut of common printers. A perfect spectral reproduction is typically not realizable and spectral gamut mapping[10] is necessary. The inversion problem can be described by a constrained optimization problem: minimize the difference between a desired reflectance spectrum and

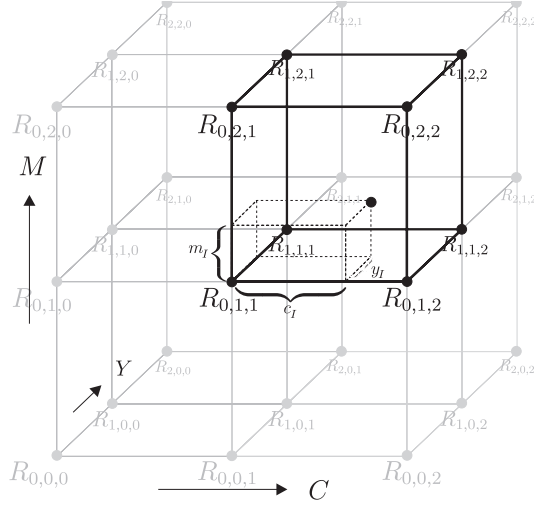the model prediction subject to ink constraints of the device.

Figure 1. CYNSN model for a CMY printer.

To invert the simple YNSN model various approaches have been proposed using standard numerical optimization techniques [11,12,13,14].

Urban et al.[15] proposed the Linear Regression Iteration (LRI) method that uses some special properties of the YNSN model and consist mainly in two simple matrix-vector multiplications. Here, the LRI method is extended to a CYNSN model.

In the following, discrete spectra are used, sampling at N wavelengths, so that each reflectance is a N dimensional vector.

The CYNSN Model

The CYNSN model is based on a subdivision of the colorant cube into smaller cuboid cells (see Figure 1). In order to fit the model to the printer the control values representing the cell vertices are typically printed and the corresponding reflectance spectra measured.

For a printer with m colorants a CYNSN model with k grid points in each dimension has $(k-1)^m$ cells. Each cell has 2^m vertices that we denote in the control value space by

$$v_{I_0},\ldots,v_{I_{2^{m-1}}} \in [0,1]^m$$

and in reflectance space by

$$R_{I_0},\ldots,R_{I_{2^{m-1}}} \in [0,1]^N$$

Here $I \in \{0,\ldots,k-1\}^m$ is a multi-index describing the cell and $j = 0,\ldots,2^m - 1$ numbers the vertex within the cell. For a CMY printer this is

$$I_0 = I + (0,0,0), I_1 = I + (0,0,1),$$
$$I_2 = I + (0,1,0), I_3 = I + (0,1,1),$$
$$I_4 = I + (1,0,0), I_5 = I + (1,0,1),$$
$$I_6 = I + (1,1,0), I_7 = I + (1,1,1)$$

In Figure 1 the cell $I = (0,1,1)$ is emphasized.

The CYNSN model for a CMY printer is defined as follows

$$R(C,M,Y) = \left(\sum_{i=1}^{8} a_{I_i}(C,M,Y) \cdot R_{I_i}^{1/n} \right)^n$$

where I is the multi-index corresponding to the cell that contains the C,M,Y values, n is the so called Yule-Nielsen factor empirically modeling the optical dot gain and a_{I_i} are the Demichel equations:

$$a_{I_0} = (1-c_I)(1-m_I)(1-y_I)$$
$$a_{I_1} = c_I(1-m_I)(1-y_I)$$
$$a_{I_2} = (1-c_I)m_I(1-y_I)$$
$$a_{I_3} = c_I m_I(1-y_I)$$
$$a_{I_4} = (1-c_I)(1-m_I)y_I$$
$$a_{I_5} = c_I(1-m_I)y_I$$
$$a_{I_6} = (1-c_I)m_I y_I$$
$$a_{I_7} = c_I m_I y_I$$

Here c_I, m_I and y_I are the effective area converges normalized to the cell size, i.e. for cyan

$$c_I = \frac{v_{I_7}^c - C}{v_{I_7}^c - v_{I_0}^c}$$

The model can be easily expanded for more than three colorants.

To use the CYNSN model the control values must be transformed initially to the effective area coverages. This is typically performed in practice through the use

of one-dimensional lookup tables.

Inverting the CYNSN Model

To invert the CYNSN model by means of minimizing RMS spectral difference to a desired spectral reflectance r the following constrained optimization problem has to be solved

$$\left\| R(C,M,Y) - r \right\|_2^2$$

subject to $0 \le C,M,Y \le 1$.

Newton-based methods are often be used to solve optimization problems, since they have a very fast convergence rate. Unfortunately the CYNSN model is not differentiable on the cell edges, so Newton-based methods can not be used without modifications to guaranty the descent transition between cells. An additional drawback of Newton-based methods is the expense of calculating the Hesse-matrix, and solving a linear equation system in each iteration step. To overcome the latter drawbacks and to deal with the simple linear constraints Urban et al.[15] proposed the Linear Regression Iteration (LRI) method.

The LRI Method

The LRI method was designed to invert the YNSN model. The method utilizes the multi-linearity of the YNSN in $1/n$ space, i.e. for each colorant the model can be decomposed linearly in $1/n$ space. For the cyan colorant of a CMY printer the YNSN model can be written as follows:

$$R(C,M,Y)^{1/n} = A_c(M,Y) \cdot C + B_c(M,Y)$$

where $A_c(M,Y)$ and $B_c(M,Y)$ are N dimensional vectors that are not dependent on cyan. For magenta and yellow similar decompositions of the model can be made. After setting the decomposed model equal to the given reflectance spectrum in $1/n$ space, the equation can be solved for cyan by simple linear regression:

$$r^{1/n} = A_c(M,Y) \cdot C + B_c(M,Y)$$

$$C = \frac{A_c(M,Y)^T \left(r^{1/n} - B_c(M,Y) \right)}{A_c(M,Y)^T A_c(M,Y)}$$

For fixed magenta and yellow the calculated cyan is the optimal value in the sense of the minimal RMS spectral difference in the $1/n$ space.

Iterating this equation by successively recalculating the colorants and considering the constraint leads to the LRI algorithm with starting point (C^0, M^0, Y^0)

REPEAT {

$$C^{i+1} = F\left[\frac{A_c(M^i,Y^i)^T \left(r^{1/n} - B_c(M^i,Y^i) \right)}{A_c(M^i,Y^i)^T A_c(M^i,Y^i)} \right]$$

$$M^{i+1} = F\left[\frac{A_m(C^{i+1},Y^i)^T \left(r^{1/n} - B_m(C^{i+1},Y^i) \right)}{A_m(C^{i+1},Y^i)^T A_m(C^{i+1},Y^i)} \right]$$

$$Y^{i+1} = F\left[\frac{A_y(C^{i+1},M^{i+1})^T \left(r^{1/n} - B_y(C^{i+1},M^{i+1}) \right)}{A_y(C^{i+1},M^{i+1})^T A_y(C^{i+1},M^{i+1})} \right]$$

$i = i+1$

UNTIL TERMINATION

Here the function F is defined as follows:

$$F[X] = \begin{cases} 0, X < 0 \\ 1, X > 1 \\ X, \text{otherwise} \end{cases}$$

Termination criteria are proposed in Urban et al.[15] where also a complexity estimation is given. For practical implementation the calculation of $A_c(M,Y)$, $B_c(M,Y)$, $A_m(C,Y)$, $B_m(C,Y)$, $A_y(C,M)$ and $B_y(C,M)$ can be performed as a matrix-vector multiplication, i.e. for $A_c(M,Y)$

$$A_c(M,Y) = A_c \cdot x(M,Y)$$

The $Nx2^{m-1}$ dimensional matrix A_c needs to be calculated only once, by simply expanding and rearranging the YNSN model. The 2^{m-1} dimensional vector $x(M,Y)$ is newly calculated for each iteration step, i.e.

$$x(M,Y) = (1,M,Y,MY)^T$$

For the other vectors $B_c(M,Y)$,

$A_m(C,Y)$, $B_m(C,Y)$, $A_y(C,M)$ and $B_y(C,M)$ the implementation can be done similarly.

Expanding the LRI method for printers with more than three colorants is straightforward.

The advantage of the LRI method compared to Newton-based methods is its simplicity. For each iteration step only two matrix-vector multiplications are performed. There is no need to calculate gradients or Hesse matrices or to solve linear equation systems.

The CLRI Method

To invert the CYNSN model the transition of the iteration from one cell to a neighboring cell is of special interest. The proposed approach is based on the LRI method described in the previous section. By holding $(m-1)$ colorants fixed, the LRI method finds in each iteration step the optimal remaining colorant, in the sense of the minimal spectral RMS error in $1/n$ space. The idea of the cellular LRI (CLRI) method is similar: In each iteration step $(m-1)$ colorants are held fix, and only the remaining colorant is optimized. The domain of this colorant includes $(k-1)$ cells. Within this domain, only $(k-1)$ linear regressions need to be performed. Each linear regression consists primarily of two matrix-vector multiplications. To allow fast access to the precalculated matrices a scheme can be created as follows:

Each cell is numbered with the multi-index I and contains a plain YNSN model. For each cell I of a CYNSN model describing a CMY printer the following matrices can be calculated in advance, as described for the LRI method, and arranged to a $Nx(m \cdot 2^m)$ matrix

$$AB^I = [A_c^I, B_c^I, A_m^I, B_m^I, A_y^I, B_y^I]$$

Here the primaries of the cell I are used in place of the Neugebauer primaries.

By ordering all of these matrices according their multi-indices leads to the following matrix scheme:

$$AB = \begin{bmatrix} AB^{(0,0,0)} \\ AB^{(0,0,1)} \\ \vdots \\ AB^{(0,0,k-2)} \\ AB^{(0,1,0)} \\ \vdots \\ AB^{(k-2,k-2,k-2)} \end{bmatrix}$$

The final matrix AB has the dimension $(N \cdot (k-1)^m)x(m \cdot 2^m)$.

The base algorithm of the CLRI method is similar to the LRI method. Only the calculation of the optimal colorant in an iteration step is replaced to consider more than one cell. Here, the method for the colorant cyan is described. For the plain YNSN model the following formula has to be calculated for the LRI method in each iteration step (see previous section):

$$C^{i+1} = F\left[\frac{A_c(M^i,Y^i)^T \left(r^{1/n} - B_c(M^i,Y^i)\right)}{A_c(M^i,Y^i)^T A_c(M^i,Y^i)} \right]$$

This formula is replaced by the following procedure, where I is the multi-index of the cell containing the actual C^i, M^i, Y^i values.

FOR $(j = 0; j < k-1; j = j+1)$
{
$$c_I^{i+1} = F\left[\frac{A_c^I(m_I^i,y_I^i)^T \left(r^{1/n} - B_c^I(m_I^i,y_I^i)\right)}{A_c^I(m_I^i,y_I^i)^T A_c^I(m_I^i,y_I^i)} \right];$$

IF $c_I^{i+1} = 0$
　　IF $I \neq (*,*,0)$
　　　　$I = I - (0,0,1)$;
　　ELSE BREAK;
ELSE
　　IF $c_I^{i+1} = 1$
　　　　IF $I \neq (*,*,k-2)$
　　　　　　$I = I + (0,0,1)$;
　　　　ELSE BREAK;
　　ELSE BREAK;
}

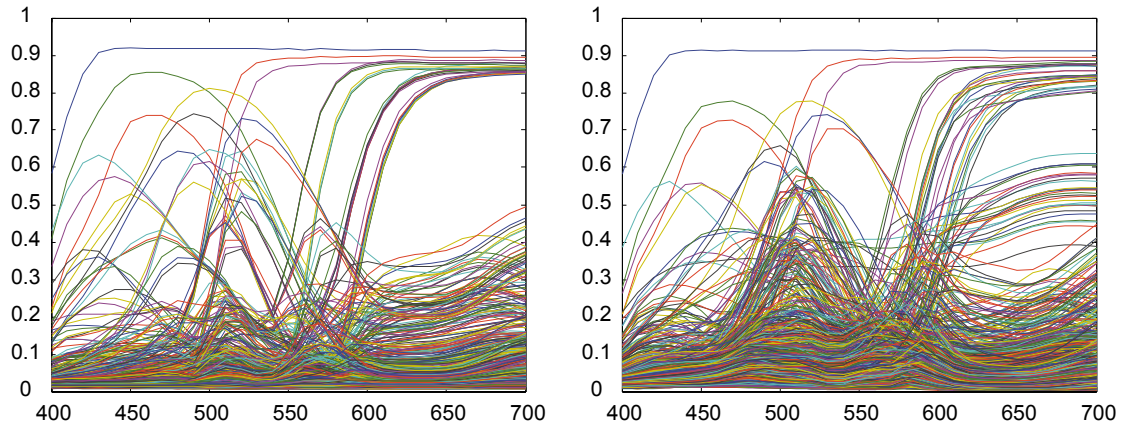For the other colorants the procedure is similar.

Figure 2 left: Cell primaries of a three grid point CYNSN model for the Mutoh Falcon 2 printer and right for the HP Designjet Z3100

By using the matrix scheme AB for each colorant. the above procedure accesses matrices in the same columns. The transition from one cell to its neighbor is simply performed through seeking to the corresponding rows. The whole iteration is performed with normalized colorants. There is no need to calculate the actual colorants from the normalized colorants during the iteration. After the sequence converges the resulting normalized control values are then converted to the real effective control values, i.e. for cyan

$$C = v_{I_7}^c \quad (v_{I_7}^c \quad v_{I_0}^c)c_I$$

Results

The CLRI method was tested using the cellular primaries of two printers: The *Mutoh Falcon II* printer and the *HP Designjet Z3100 Photo* printer. .Using the raster image processor (RIP) software *Onyx ProductionHouse*, 6 colorants of the Mutoh printer and 7 colorants of the HP printer were independently controlled. For this test 6 colorants for both printers were used. For the Mutoh printer, CMYKOG were used and for the HP printer the CMYKRG ink set was used. The number of grid points used for the CYNSN model was 3 for both printers. Additionally, a 4, grid point CYNSN model was analyzed for the HP printer. The grid point positions were optimized according Chen et al.[9]. The Yule-Nielsen n-factor for the Mutoh printer was 10 and for the HP printer 8. Both

were optimized by means of the colorant ramps.

The aim of this experiment was to validate the speed of convergence of the CLRI method and the accuracy of the results in terms of colorimetric and spectral RMS errors. Since the accuracy of the CYNSN model were out of the scope of this paper, each CYNSN model was considered to be accurate in his forward implementation.

Only in-gamut spectra were considered for this analysis since the spectral gamut mapping minimizing the RMS difference in $1/n$ space, implicitly made by the CLRI method, often achieves visually poor results. Other research is looking at gamut mapping methods that are better related to human color vision.

To ensure that only spectral reflectances within the spectral gamut of the printers were included, 1 million control values, with digital counts $\{0, 13, 20, 29, 44, 64, 92, 131, 184, 255\}^6$ were selected with corresponding reflectance spectra computed by using the forward CYNSN model. The resulting reflectances were by construction within the spectral gamut of the printer and used to test the CLRI method. The value $(0, 0, 0, 0, 0, 0)^T$ was used as the starting point of the CLRI search.

Table 1-3 show the colorimetric and spectral accuracy. ΔE_{00}^* values for three different illuminants CIE A, CIE D50 and CIE F11 were calculated.

	mean	std	max
ΔE_{00}^* (A)	0.61	0.48	6.1
ΔE_{00}^* (D50)	0.69	0.65	10.1
ΔE_{00}^* (F11)	0.66	0.57	9.2
RMS	0.004	0.004	0.054

Table 1. CLRI accuracy for the Mutoh printer

	Mean	std	max
ΔE_{00}^* (A)	0.38	0.88	15.8
ΔE_{00}^* (D50)	0.39	0.93	15.9
ΔE_{00}^* (F11)	0.45	0.93	13.5
RMS	0.002	0.004	0.092

Table 2. CLRI accuracy for the HP printer (3 grid points)

	mean	std	max
ΔE_{00}^* (A)	0.27	0.69	18.9
ΔE_{00}^* (D50)	0.27	0.68	19.8
ΔE_{00}^* (F11)	0.31	0.68	20.39
RMS	0.0019	0.004	0.088

Table3. CLRI accuracy for the HP printer (4 grid points)

Here the spectral RMS difference between two spectral reflectances r_1 and r_2 is calculated as follows:

$$RMS(r_1, r_2) = \frac{\|r_1 - r_2\|_2}{\sqrt{N}}$$

The average number of linear regressions needed for one inversion is shown in Table 4

	Average number of linear regression / inversion
Mutoh	332
HP (3 grid points)	247
HP (4 grid points)	492

Table4. Average number of linear regressions / inversion

Discussion

The results showed that the CLRI method converges to reflectance spectra that are on average not distinguishable from the original. The mean and standard deviation of the ΔE_{00}^* color differences were far below 1. The large maximal color differences result from very dark samples, where small spectral RMS distances can result in huge color differences. Since the method minimizes the spectral RMS distances in $1/n$ space, large color errors can be the consequence. Therefore it is important to consider additional constraints for very dark spectra.

The number of average linear regressions computed for one inversion seems high. The cause for this is the choice of the starting point in combination with the choice of the test spectra. The investigated spectra are mainly located in the dark area of the gamut, so many transitions between cells are necessary to reach the right cell. In practice it is not necessary to select a fixed starting point. For the reproduction of multispectral images, where neighboring pixels have in general high correlation, the starting points can depend on the previous calculation. So e.g. the resulting control value of the previous neighboring pixel can be chosen as the starting point of the current pixel inversion. With this technique the transitions between cells can be minimized and therefore the number of linear regressions. It should be noticed that linear regression for the CLRI method consists mainly of only two matrix-vector multiplications.

Conclusion

The Linear Regression Iteration (LRI) technique has been proposed for inversion of the cellular Yule-Nielson spectral Neugebauer (CYNSN) model. Each iteration consists mainly of only two simple matrix-vector multiplications. The matrices can be calculated in advance and arranged in a matrix scheme. The transition of the iteration from one cell to the neighboring cell is performed by choosing the right matrix from the matrix scheme.

Using CYNSN models of two six-colorant printers the

performance of the method concerning colorimetric and spectral RMS accuracy and speed of convergence was investigated. The average accuracy was far below the just noticeable color difference. For very dark colors maximal colorimetric error can be high, even if the spectral RMS errors are small. To overcome this systematic drawback, additionally constraints need to be considered for dark colors.

Acknowledgements

References

1. D. R. Wyble and R. S. Berns. A Critical Review of Spectral Models Applied to Binary Color Printing. Color Research and Application, 25:4-19, (2000).

2. H. E. J. Neugebauer. Die theoretischen Grundlagen des Mehrfarbenbuchdrucks. Zeitschrift für wissenschaftliche Photographie, Photophysik und Photochemie, 36:73-89, (1937).

3. H. E. J. Neugebauer. The Theoretical Basis of Multicolor Letterpress Printing (Translated D. Wyble and A. Kraushaar). Color Research and Application, 30:322-331, (2005).

4. J. A. C. Yule and W. J. Nielsen. The penetration of light into paper and its effect on halftone reproduction. In Tech. Assn. Graphic Arts, volume 4, pages 65-76, (1951).

5. J. A. C. Yule and R. S. Colt. Colorimetric Investigations in Multicolor Printing. In TAGA Proceedings, pages 77-82, (1951).

6. J.A.S. Viggiano. The Color of Halftone Tints. In TAGA Proceedings, pages 647-661, (1985).

7. J.A.S. Viggiano. Modeling the Color of Multi-color Halftones. In TAGA Proceedings, pages 44-62, (1990).

8. K. J. Heuberger, Z. M. Jing and S. Persiev. Color Transformations from Lookup Tables. In TAGA Proceedings, pages 863–881, (1992).

9. Six color printer characterization using an optimized cellular Yule- Nielsen spectral Neugebauer model Author: Chen, Y.; Berns, R.S.; Taplin, L.A. J. Imag. Sci. Tech. 48, 519-528, (2004)

10. M. R. Rosen and M. W. Derhak, Spectral Gamuts and Spectral Gamut Mapping, Proc. SPIE 6062, (2006).

11. S. Zuffi and R. Schettini. Spectral-Based Printer Characterization. In CGIV, pages 598-602, Poitiers, France, (2002).

12. L. A. Taplin. Spectral Modeling of a Six-Color Inkjet Printer, MSc. thesis. RIT,NY, 2001. MSc. thesis. RIT, NY, (2001).

13. D.-Y. Tzeng. Spectral-Based Color Separation Algorithm Developed for Multiple-Ink Color Reproduction. PhD thesis. (1999).

14. D.-Y. Tzeng and R. S. Berns. Spectral-Based Six-Color Separation Minimizing Metamerism. In IS&T/SID, pages 342-347, Scottsdale Ariz., (2000).

15. P. Urban and R.-R. Grigat. Spectral-Based Color Separation using Linear Regression Iteration. Color Research and Application, 31:229-238, (2006).